

NONEQUILIBRIUM FLUCTUATIONS IN ACTIVELY COOLED RESONATORS

Michele Bonaldi

Ist. di Fotonica e Nanotecnologie
CNR-Fondazione Bruno Kessler
via alla Cascata, 56/C
38100 Povo, Trento, Italy
bonaldi@science.unitn.it

Livia Conti

Ist. Nazionale di Fisica Nucleare
Sezione di Padova
Via Marzolo 8
35131 Padova, Italy
Livia.Conti@lnl.infn.it

Paolo De Gregorio

Dipartimento di Matematica
Politecnico di Torino
Corso Duca degli Abruzzi 24
10129 Torino, Italy
paolo.degregorio@polito.it

Lamberto Rondoni

Dipartimento di Matematica
Politecnico di Torino
Corso Duca degli Abruzzi 24
10129 Torino, Italy
lamberto.rondoni@polito.it

Gabriele Vedovato

Ist. Nazionale di Fisica Nucleare
Sezione di Padova
Via Marzolo 8
35131 Padova, Italy
gabriele.vedovato@lnl.infn.it

Andrea Vinante

Ist. Nazionale di Fisica Nucleare
Sezione di Padova
Via Marzolo 8
35131 Padova, Italy
vinante@science.unitn.it

Abstract

We analyze heat and work fluctuations in the gravitational wave detector AURIGA [Zendri *et al.*, 2002], modeled as a macroscopic electromechanical oscillator in contact with a thermostat and cooled by an active feedback system. The oscillator is driven to a steady state by the feedback cooling, equivalent to a viscous force.

Key words

feedback cooling; thermal noise; gravitational waves; fluctuation relations.

1 Introduction

Cold damping feedback is effective in reducing the thermal noise induced motion of an oscillator by applying a viscous force: this has operated successfully in a wide variety of devices, from nano to macroscopic resonators, and in a variety of implementations, including both optical and electrical forces. In basic research, the cold damping is considered either to reduce the position uncertainty of macroscopic bodies due to thermal noise below the level of intrinsic quantum fluctuations, to allow the observation of quantum dynamics of these systems [Aspelmeyer and Schwab, 2008], or to improve the behavior of future gravitational wave detectors [Mancini *et al.*, 1998], where displacement measurements with uncertainty at the Heisenberg limit will be at reach.

It is customary to assume the cold-damped oscillator equivalent to a higher-loss one, in thermodynamic equilibrium at a fictitious temperature T_{eff} smaller than T_0 ,

the thermodynamic temperature of the bath which it is in contact with. By contrast in this work, we aim to reveal the nonequilibrium nature of the steady states of our cold-damped oscillator, and to characterize the fluctuations of its thermodynamic observables.

In the past 15 years, a large number of works has been devoted to similar problems. In particular, the Fluctuation Relation (FR) concerning the entropy production rate in deterministic systems, which was obtained in Ref. [Evans *et al.*, 1993] and was further developed e.g. in Ref.s [Evans and Searles, 1994; Gallavotti and Cohen, 1995; Rondoni *et al.*, 2000; Searles *et al.*, 2007; Bonetto, 2006], motivated similar studies in stochastic systems, of interest in our investigation. Ref. [Kurchan, 1998] concerns Langevin dynamics with an external deterministic driving term and leads to a FR closely analogous to the one of Ref. [Evans *et al.*, 1993]. Reference [Harris *et al.*, 2006; Baiesi, 2006; Visco, 2006] considers possible alternative scenarios. The result of these, as well as of many other theoretical studies, is that the FR for some properly identified observable (called dissipation function) is quite generally valid in systems of physical interest. Hence the FR has become a standard tool to characterize nonequilibrium systems. Indeed, various experimental tests confirmed this view, see Ref. [Wang *et al.*, 2002] for dragged colloidal particles, Ref. [Garnier and Ciliberto, 2005] for electrical circuits and Ref. [Douarche *et al.*, 2006; Joubaud *et al.*, 2007] for mechanical oscillators.

In these works, the nonequilibrium state is caused by an external, deterministic agent. Differently, thanks to the feedback cooling, here for the first time we study experimentally an oscillator driven by

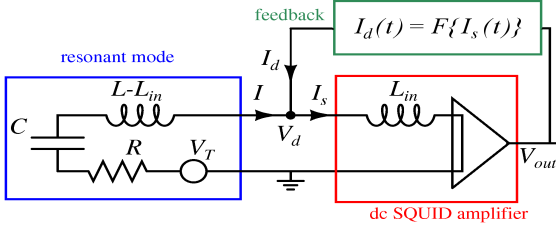


Figure 1. The normal mode is approximated, around its resonance frequency, by a series-RLC circuit. The dc SQUID is represented as current amplifier with two noise sources, which can be neglected at moderate feedback gains. The observable is the current I_s , and the electronic feedback cooling is obtained by sending back a current I_d which is a delayed copy of I_s reduced by $G \ll 1$. The SQUID output voltage is $V_{out} = AI_s$ with $A = 2.6 \cdot 10^6 \Omega$.

a stochastic force, a situation investigated theoretically in Ref.s [Farago, 2002; Kim and Quian, 2007], where however opposite conclusions about the FR were reached. In our case the force is due to an external agent equivalent to a viscous force, which breaks the time reversibility of the equation of motion. Our results reveal that AURIGA is away from equilibrium and that our Langevin model describes correctly its fluctuations (see also Ref. [Bonaldi, 2009]). The fluctuations of the injected power are in good agreement with the analytical calculation performed in Ref. [Farago, 2002].

2 The experimental system

AURIGA is based on a 2.2×10^3 kg, 3 m long bar made of a low loss aluminum alloy (Al5056), cooled to liquid helium temperatures $T_0 = (4.6 \pm 0.2)$ K. The fundamental longitudinal mode of the bar, sensitive to gravitational waves, has effective mass $M=1.1 \times 10^3$ kg and resonance frequency $\omega_0/2\pi \sim 900$ Hz. The bar resonator motion is detected by a capacitive sensor followed by a double stage dc-SQUID amplifier; the displacement sensitivity is about $5 \cdot 10^{-20}$ m/ $\sqrt{\text{Hz}}$ over a ~ 100 Hz bandwidth around ω_0 , largely limited by thermal noise. The detector can be modeled by three coupled low-loss resonators: two mechanical ones (the bar itself and a plate of the capacitive transducer) and an LC electrical one, whose dynamics is well described by three normal modes at separate frequencies, each being a mixture of the electrical and mechanical resonators [Vinante *et al.*, 2002; Baggio *et al.*, 2005]. A mode can be modeled as a RLC series electrical oscillator with an effective inductance L , capacitance C and resistance R which assume different values for the 3 oscillators (Figure 1). To the sole purpose of improving the electronics stability and easing the data analysis, AURIGA employs an electronic feedback cooling scheme on the detector, which is equivalent to a viscous force that damps the oscillators [Vinante *et al.*, 2008].

2.1 Langevin model

The dynamics of each electromechanical oscillator, at moderate feedback gains, is well approximated by (see Fig. 1):

$$(L - L_{in}) \frac{d^2 q(t)}{dt^2} + R \frac{dq(t)}{dt} + \frac{q(t)}{C} = V_T(t) - V_d(t) \quad (1a)$$

$$V_d(t) = L_{in} \frac{dI_s(t)}{dt} \quad (1b)$$

$$I(t) + I_d(t) = I_s(t) \quad (1c)$$

$$I(t) = \frac{dq(t)}{dt} \quad (1d)$$

where the observable is the output current I_s and the noise due to the SQUID amplifier is neglected. In thermodynamic equilibrium, each oscillator is driven by the stochastic voltage $V_T(t) = \sqrt{2k_B T_0 R} \Gamma(t)$, where Γ is a Gaussian white process. This should hold even in our nonequilibrium case, since the feedback cooling concerns only 3 modes, out of the very many degrees of freedom of the thermal bath, and is not expected to affect significantly the thermal noise arising from the interaction with the bath. The feedback current I_d is chosen to be:

$$I_d(t) = GI_s(t - t_d) \quad (2)$$

where $t_d = \frac{\pi}{2\omega_r}$, $\omega_r = 1/\sqrt{LC}$ is the oscillator's resonant angular frequency and $G \ll 1$ [Vinante *et al.*, 2008]. This choice produces a feedback force equivalent to a viscous damping.

Equation (1b) includes memory effects, due to contributions from times $t - t_d$, because of the constraints (1c) and (2). However, thanks to the very low losses of the oscillators, the currents I_s , I_d and I oscillate at ω_r with amplitude and phase changing appreciably only on timescales of several cycles. Thus, the quasi-harmonic approximation $I(t) = \hat{I}(t) \sin[\omega_r t + \phi(t)]$, like the analogous ones for I_s and I_d , seems appropriate. In this approximation, each oscillator obeys:

$$L \frac{dI_s(t)}{dt} + I_s(t) [R + R_d] + \frac{q_s(t)}{C} = \sqrt{2k_B T_0 R} \Gamma(t) \quad (3a)$$

$$I_s(t) = \frac{dq_s(t)}{dt} \quad (3b)$$

where $R_d = G\omega_r L_{in}$ expresses the viscous damping on the oscillator due to the feedback loop and the memory effects are accounted for via the quasi-harmonic approximation; the feedback efficiency is defined as $g = R_d/R$. Equation (3) is not invariant under time reversal ($q'_s = q_s$, $I'_s = -I_s$, $t' = -t$) and does not satisfy the Einstein relation. Nevertheless, it is formally identical to that describing an oscillator with damping

$R + R_d$, in equilibrium at the fictitious *effective temperature* $T_{eff} = T_0/(1 + g)$. The discrepancy between T_{eff} and the thermal bath temperature T_0 reveals the nonequilibrium nature of the phenomenon. Hence, the feedback cooled oscillator is usually treated as an equilibrium system, with T_{eff} derived from the experimental value of $\langle \hat{I}_s^2(t) \rangle = 2 \frac{k_B T_{eff}}{L}$, even if no bath at T_{eff} is present. Operating on the feedback gain, we have thus achieved a temperature as low as 0.17 mK, for the coldest of our 3 oscillators [Vinante *et al.*, 2008].

2.2 Energy balance

Multiplying Eq. (3a) by $I_s(t)$ and integrating between t and $t + \tau$, in the quasi-harmonic approximation we get an expression for the average power $P_\tau = \frac{1}{\tau} \int_t^{t+\tau} I_s(t') V_T(t') dt'$ injected by the stochastic thermal force during a time τ :

$$P_\tau = \frac{U(t + \tau) - U(t)}{\tau} + \frac{R + R_d}{\tau} \int_t^{t+\tau} I_s^2(t') dt' \quad (4)$$

where $U(t)$ is the energy stored in the oscillator:

$$U(t) = \frac{1}{2} L I_s^2(t) + \frac{1}{2} \frac{q_s^2(t)}{C} = \frac{1}{2} L \hat{I}_s^2(t) \quad (5)$$

The term proportional to R represents the heat dissipated by the oscillator toward the bath while the term proportional to R_d is the work done by the oscillator on the feedback:

$$W_\tau = -\frac{1}{\tau} \int_t^{t+\tau} I_d(t') V_d(t') dt' = \frac{1}{\tau} R_d \int_t^{t+\tau} I_s^2(t') dt' \quad (6)$$

Notice that the last identity is strictly valid only within the quasi-harmonic approximation, which relates both $I_s(t - t_d)$ and $dI_s(t)/dt$ to the instantaneous current $I_s(t)$. Further, if τ is a multiple of the period ($\tau = N \frac{2\pi}{\omega_r}$, N integer), in the same approximation we can also write:

$$W_\tau = \frac{1}{\tau} \frac{R_d}{2} \int_t^{t+\tau} \hat{I}_s^2(t') dt' \quad (7)$$

Conservation of energy implies that the heat Q_τ absorbed by the oscillator from the bath averaged in the time τ is:

$$Q_\tau = \frac{U(t + \tau) - U(t)}{\tau} + W_\tau \quad (8)$$

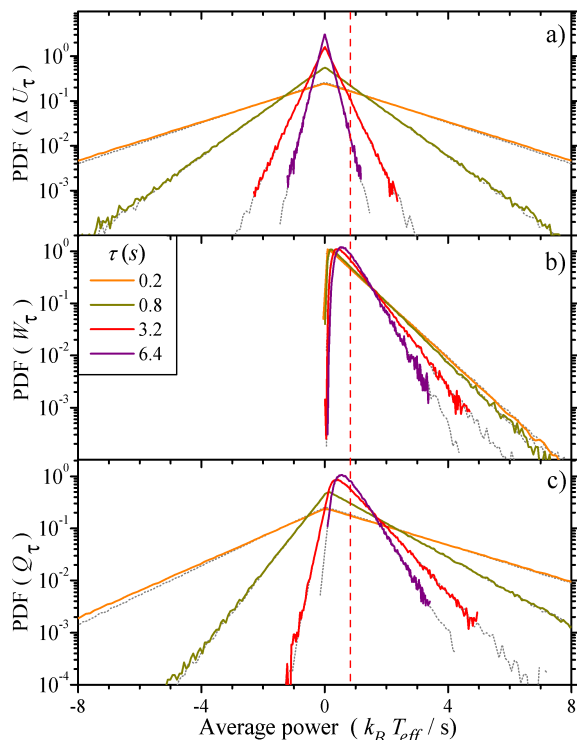


Figure 2. PDF (units of $s/(k_B T_{eff})$) of: (a) the time averaged energy difference $[U(t + \tau) - U(t)]/\tau$, (b) the work W_τ and (c) the heat Q_τ averaged over $\tau = 0.2, 0.8, 3.2, 6.4$ s. Dashed vertical line corresponds to $0.84 k_B T_{eff}/s$. The plots show the data collected by AURIGA in an uninterrupted 10 days time span. We show also (gray dotted lines) the curves obtained by numerical simulation of Eq. (3) for a 50 days time span. The discrepancies observed at short τ between experimental and numerical data are within the uncertainty due to the experimental error in τ_{eff} .

3 Experimental results

To study nonequilibrium properties, we decided to focus only on the lowest frequency mode out of the 3: this mode is well separated in frequency from the other two and it is thus our best approximation of a single oscillator. The experimental data cover a continuous 10 days time span and were acquired in march 2008. The sampled current $\hat{I}_s(t)$ was processed via the standard AURIGA data analysis and integrated over the resonance to obtain the current amplitude $\hat{I}_s(t)$ in the harmonic approximation. Averaging over several reading of a thermometer placed on the bar gives us $T_0 = (4.6 \pm 0.2)$ K and from dedicated calibration of the AURIGA detector we measure $L = (1.67 \pm 0.01) 10^{-4}$ H and $L_{in} = (1.48 \pm 0.01) 10^{-6}$ H. We measure from the experimental data $\omega_r/2\pi = 865.7$ Hz, decay time $\tau_{eff} = (2.36 \pm 0.04)$ s and $T_{eff} = (21.1 \pm 0.2)$ mK; hence we estimate $g = 207 \pm 10$, $R = (6.8 \pm 0.5) 10^{-7}$ Ω and $G = (1.74 \pm 0.06) 10^{-2}$. In Figure 2a and 2b we show the Probability Density Function (PDF) of the energy difference and of the work done by the oscillator averaged over growing time intervals τ : they are calculated from Eqs. (5) and (7) after dividing the experimental data in contiguous time intervals of duration τ . In Fig-

ure 2c we show the corresponding heat exchanged by the oscillator with the bath averaged over different time intervals τ and computed via the energy conservation Eq.(8). The fluctuations of the heat are asymmetric as expected for a nonequilibrium steady state. We do not show the PDF of the injected power P_τ , evaluated by Eq. (4), as they are essentially identical to those of Q_τ , since $P_\tau \approx Q_\tau$ when $g = R_d/R \gg 1$.

The PDF of the time averaged energy difference is symmetric with respect to zero as for an equilibrium oscillator. It has exponential tails which decay faster for longer τ . The time averaged work, which is positive, has a highly asymmetric PDF and from Eq. (7) and the formal (equilibrium) energy equipartition theorem we expect it to have constant mean given by $R_d \frac{k_B T_{eff}}{L} \simeq 0.84 k_B T_{eff}/s$. As a consequence, the time averaged absorbed heat assumes negative values only for short integration times, with the characteristic time scale given by cold damped oscillator decay time $\tau_{eff} = 2L/(R+R_d)$: for $\tau \gg \tau_{eff}$ the contribution of the time averaged energy becomes negligible. So in the presence of feedback ($R_d > 0$) there is a net heat transfer from the bath to the oscillator: this is precisely the energy flux that feeds the nonequilibrium steady state. On the contrary, for $R_d = 0$ the heat equals the energy difference and its PDF is symmetric with respect to its (zero) mean value; the feedback modifies the PDF of the heat making it highly asymmetric.

4 Discussion

This model constitutes only a partial thermodynamic description of the experimental apparatus, since we do not account for the entropy produced by the feedback scheme. So we have actually modeled a *Maxwell demon* [Leff and Rex, 2003], which uses the measurements of I_s to convert heat from a single heat bath to work. It is widely accepted that demons do not break the second law when they are fully accounted for. We evidence at least two phenomena not considered in our model: the energy dissipation due to the current flowing in the feedback network and the entropy produced by the erasure of the previous information in the measurement process [Landauer, 1961]. The former does not give rise to a fundamental contribution: it depends on the specific circuit used to implement the feedback current Eq. (2) and might be made negligible in respect to W_τ . On the contrary the latter is unavoidable; an analysis of information entropy in feedback systems has been recently addressed for flashing ratchet systems [Cao, Feito and Touchette, 2009], but no results are currently available for cold-damped systems.

For this reason we think that our thermodynamic observables cannot be directly identified with the dissipation function of the FR. On the other hand we cannot test the FR for the alternative dissipation function suggested in Ref. [Kim and Quian, 2007] since this requires access to extremely rarely populated tails of the PDFs. However the situation described by Eqs. (3) and

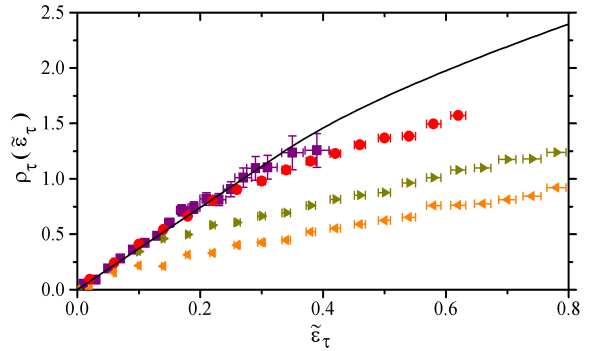


Figure 3. Plot of $\rho_\tau(\tilde{\epsilon}_\tau)$ for $\tau=0.2$ s (\blacktriangleleft), 0.8 s (\blacktriangleright), 3.2 s (\bullet), 6.4 s (\blacksquare). Solid line is the prediction of Eq. (9). Vertical errors come from statistic uncertainty, while horizontal errors are mainly due to the measurement resolution of τ_{eff} ; error bars are not plotted when smaller than the size of the symbol. As expected, the agreement with the theory improves with growing τ .

(7) has been considered in Ref.[Farago, 2002] where the large deviation function of the injected power P_τ is derived. If $\tau \gg \tau_{eff}$, the PDF of P_τ was proved to satisfy the relation:

$$\begin{aligned} \rho_\tau(\tilde{\epsilon}_\tau) &\equiv \frac{1}{\tau} \ln \frac{\text{PDF}(\tilde{\epsilon}_\tau)}{\text{PDF}(-\tilde{\epsilon}_\tau)} \\ &= \begin{cases} 4\gamma\tilde{\epsilon}_\tau, & \text{if } \tilde{\epsilon}_\tau < \frac{1}{3}; \\ \gamma\tilde{\epsilon}_\tau \left(\frac{7}{4} + \frac{3}{2\tilde{\epsilon}_\tau} - \frac{1}{4\tilde{\epsilon}_\tau^2} \right), & \text{if } \tilde{\epsilon}_\tau \geq \frac{1}{3}. \end{cases} \quad (9) \end{aligned}$$

where $\tilde{\epsilon}_\tau = P_\tau L/(k_B T_0 R)$ is the reduced injected power and $\gamma = (R+R_d)/L = 2/\tau_{eff}$. Figure 3 shows the experimentally measured ρ_τ together with the theoretical prediction Eq. (9). The agreement with the theory improves at longer τ , even if the experimental errors grows because large negative values of $\tilde{\epsilon}_\tau$ becomes extremely rare. With the current amount of experimental data, we were able to test the theoretical predictions up to $\tau = 6.4$ s; a more accurate study on a set of 3 years of data is ongoing. An experimental test of Eq. (9) has also been recently obtained in wave turbulence [Falcon *et al.*, 2008]. We point out that Eq. (9) differs greatly from the work fluctuations in a forced torsional oscillator reported in Ref. [Douarche *et al.*, 2006; Joubaud *et al.*, 2007]. In that case, a periodic forcing was applied and therefore it was possible to develop a complete thermodynamic model of the experiment: hence the proper dissipation function was identified and the FR was tested successfully.

Acknowledgements

The research leading to these results has received funding from the European Research Council under the European Community's Seventh Framework Programme (FP7/2007-2013) / ERC grant agreement n. 202680.

References

- Aspelmeyer, M. and Schwab, K. C. (2008) *New J. Phys.*, **10**, 095001.
- Baggio, L., *et al.* (2005) 3-Mode detection for widening the bandwidth of resonant gravitational wave detectors. *Phys. Rev. Lett.*, **94**, 241101.
- Baiesi, M., *et al.* (2006) Fluctuation symmetries for work. *Phys. Rev. E*, **74**, 021111.
- Bonaldi, M., *et al.* (2009) Nonequilibrium steady state fluctuations in actively cooled resonators. *Phys. Rev. Lett.*, **103**, 010601.
- Bonetto, F., *et al.* (2006) Chaotic hypothesis, fluctuation theorem, singularities. *J. Stat. Phys.*, **123**, pp. 39–54.
- Cao, F. J., Feito, M., Touchette, H. (2009) Information and flux in a feedback controlled Brownian ratchet. *Physica A*, **338**, pp. 113–119.
- Douarche, F., *et al.* (2006) Work fluctuation theorems for harmonic oscillators. *Phys. Rev. Lett.*, **97**, 140603.
- Evans, D. J. Cohen, E. G. D. and Morriss, G. P. (1993) Probability of second law violations in shearing steady flows. *Phys. Rev. Lett.*, **71**, pp. 2401–2404.
- Evans D. J. and Searles D. J. (1994) Equilibrium microstates which generate second law violating steady states. *Phys. Rev. E*, **50**, pp. 1645–1648.
- Falcon, É., *et al.* (2008) Fluctuations of energy flux in wave turbulence. *Phys. Rev. Lett.*, **100**, 064503.
- Farago, J. (2002) Injected power fluctuations in Langevin equation. *J. Stat. Phys.*, **107**, pp. 781–803.
- Gallavotti, G. and Cohen, E. G. D. (1995) Dynamical ensembles in stationary states. *J. Stat. Phys.*, **80**, pp. 931–970.
- Garnier, N. and Ciliberto, S. (2005) Nonequilibrium fluctuations in a resistor. *Phys. Rev. E*, **71**, 060101(R).
- Harris, R. J., *et al.* (2006) Breakdown of Gallavotti-Cohen symmetry for stochastic dynamics. *Europhys. Lett.*, **75**, pp. 227–233.
- Joubaud, S., *et al.* (2007) Fluctuation theorems for harmonic oscillators. *J. Stat. Mech.*, P09018.
- Kim, K. H. and Qian, H. (2007) Fluctuation theorems for a molecular refrigerator. *Phys. Rev. E*, **75**, 022102.
- Kurchan, J. (1998) Fluctuation theorem for stochastic dynamics. *J. Phys. A*, **31**, pp. 3719–3729.
- Landauer, R. (1961) Irreversibility and heat generation in the computing process. *IBM J. Res. Dev.*, **5**, pp. 183–191.
- Leff, H. S. and Rex, A. F., (eds.) (2003) *Maxwell's Demon 2* (Institute of Physics, Bristol).
- Mancini, S., Vitali, D. and Tombesi, P. (1998) Optomechanical cooling of a macroscopic oscillator by homodyne feedback. *Phys. Rev. Lett.*, **80**, pp. 688–691.
- Rondoni, L., *et al.* (2000) Fluctuation theorems for entropy production in open systems. *Phys. Rev. E*, **61**, pp. R4679–R4682.
- Searles, D. J., *et al.* (2007) The steady state fluctuation relation for the dissipation function. *J. Stat. Phys.*, **128**, pp. 1337–1363.
- Vinante, A., *et al.* (2002) Stabilization and optimization of a two-stage dc SQUID coupled to a high Q resonator. *Physica C*, **368**, pp. 176–180.
- Vinante, A., *et al.* (2008) Feedback cooling of the normal modes of a massive electromechanical system to submillikelvin temperature. *Phys. Rev. Lett.*, **101**, 033601.
- Visco, P. (2006) Work fluctuations for a Brownian particle between two thermostats. *J. Stat. Mech.*, P06006.
- Wang, G.M., *et al.* (2002) Experimental demonstration of violations of the second law of thermodynamics for small systems and short time scales. *Phys. Rev. Lett.*, **89** 050601.
- Zendri, J. P., *et al.* (2002) Status report and near future prospects for the gravitational wave detector AURIGA. *Class. Quant. Grav.*, **19**, pp. 1925–1933.